Applied Physics Letters ARTICLE scitation.org/journal/apl

Electron spin dynamics in mesoscopic GaN nanowires

Cite as: Appl. Phys. Lett. **114**, 092406 (2019); doi: 10.1063/1.5080508
Submitted: 9 November 2018 · Accepted: 15 February 2019 ·
Published Online: 8 March 2019

J. H. Buß,[1] S. Fernández-Garrido,[2,a)] O. Brandt,[2] D. Hägele,[1] and J. Rudolph[1,b)]

AFFILIATIONS

[1]Ruhr University Bochum, Faculty of Physics and Astronomy, Experimental Physics VI (AG), Bochum, Germany
[2]Paul-Drude-Institut für Festkörperelektronik, Leibniz-Institut im Forschungsverbund Berlin e.V., Hausvogteiplatz 5-7, 10117 Berlin, Germany

[a)]**Present address:** Grupo de electrónica y semiconductores, Dpto. Física Aplicada, Universidad Autónoma de Madrid, C/Francisco Tomás y Valiente 7, 28049 Madrid, Spain.
[b)]**Author to whom correspondence should be addressed:** joerg.rudolph@ruhr-uni-bochum.de

ABSTRACT

The electron spin dynamics in spontaneously formed GaN nanowires (NWs) on Si(111) is investigated by time-resolved magneto-optical Kerr-rotation spectroscopy for temperatures from 15 to 260 K. A strong increase in the electron spin relaxation time by more than an order of magnitude is found as compared to bulk GaN. The temperature dependence of spin relaxation is characterized by two regimes, which are explained by a model taking into account the coexistence of two different mechanisms. As a result, the spin lifetime is limited by hyperfine interaction of localized electron spins with nuclear spins at low temperatures. The mesoscopic electron confinement in the NWs leads to a dominance of Dyakonov-Perel spin relaxation driven by interface-induced contributions at high temperatures, resulting in a slow-down, but not complete suppression of spin relaxation as compared to bulk GaN. These findings underline the important role of the high surface-to-volume ratio in NWs.

Semiconductor electronics has evolved with impressive speed since its beginnings, leading to ever shrinking device dimensions and an explosive growth of performance. Completely new concepts for quantum mechanical semiconductor devices will, however, soon be required to maintain the current pace and to eliminate the inevitable limits of classical device concepts.[1] Spintronics as a spin-based electronics and semiconductor nanowires (NWs) are both promising candidates for such alternative approaches. Spintronics has intensively been pursued over the last few years, resulting in a deepened understanding of spin phenomena in semiconductors and numerous device proposals ranging from spin field effect transistors and spin lasers to concepts for quantum computing and communication.[2] Similarly, semiconductor NWs are vividly explored, where especially GaN NWs have attracted strong interest due to their high structural perfection.[3] A broad spectrum of GaN NW devices has already been demonstrated, including field effect transistors, photodetectors, on-chip optical interconnects, single-photon emitters, and single NW lasers.[4]

Combining the advantages of these two approaches by employing the electronic spin degree of freedom in NWs promises additional benefits.[5] In particular, for electrons confined to narrow, quasi one-dimensional semiconductor channels, theory predicts the usually dominating Dyakonov-Perel (DP) spin relaxation mechanism to be inactive, resulting in drastically reduced or even completely suppressed transport-induced spin relaxation.[6] NWs with mesoscopic confinement are expected to show not a complete suppression, but still a substantial slow-down of spin relaxation.[7] Experimental studies of spin dynamics in NWs are, however, scarce[8] as compared to the extensive work on bulk, quantum well, and quantum dot systems.[6] Furthermore, most studies have concentrated on NWs fabricated by top-down approaches from semiconductor heterostructures,[9] while NWs grown by bottom-up approaches have received less attention. In particular, the mechanisms of spin relaxation in spontaneously formed GaN NWs have not yet been elucidated, though the demonstration of electrical spin injection into GaN NWs[10] and of GaN NW-based spin lasers[11] has clearly indicated their potential.

In the present work, we investigate the electron spin dynamics in spontaneously formed, unintentional *n*-type GaN NWs on Si(111) by time-resolved magneto-optical Kerr-rotation spectroscopy (TRKR) for temperatures from 15 to 260 K. We find a nonmonotonic temperature dependence of spin relaxation which is modeled taking into account

both the hyperfine interaction of localized electron spins with nuclear spins and DP spin relaxation of delocalized electrons. The magnetic field dependence of spin relaxation allows us to identify interface-induced contributions as the driving force for DP relaxation.

The primarily investigated NW ensemble (sample A) was grown by plasma-assisted molecular beam epitaxy on a Si(111) substrate. Suitable growth conditions led to the spontaneous formation of NWs with a number density of $2 \times 10^{10}\,\mathrm{cm}^{-2}$ and a length and diameter of (450 ± 150) nm and (39 ± 14) nm, respectively [see Figs. 1(a) and 1(b)].[3] Si and O donors lead to an unintentional *n*-type background doping. TRKR measurements were performed with the frequency-doubled output of a fs-modelocked Ti:sapphire laser, which was split into pump and probe beams. The pump beam was focused down to a spot with a diameter of approximately 100 μm on the sample surface, exciting a spin-polarized electron ensemble in the GaN NWs. The temporal evolution of the initially created spin polarization was tracked via the Kerr-rotation of the linearly polarized probe pulse, which was time-delayed with respect to the pump pulse by a variable mechanical delay line. A cascaded lock-in amplifier detection scheme with polarization modulation of the pump beam was employed for sensitive detection.[12] The energy of the pump and probe was set to the maximum of the Kerr-rotation signal at each temperature, shifting from 3.48 eV at 15 K to 3.42 eV at 260 K following the temperature-induced shrinkage of the bandgap. The average power of the pump and probe was 10 and 1 mW, respectively. The samples were mounted in a cold-finger cryostat, where an external magnetic field B_{ext} was applied in the sample plane.

Figure 1(c) shows exemplarily TRKR transients at different temperatures. The transients exhibit an oscillatory behavior due to spin Larmor precession around the external magnetic field and a temporal decay of the amplitude caused by spin relaxation and, in general, also by

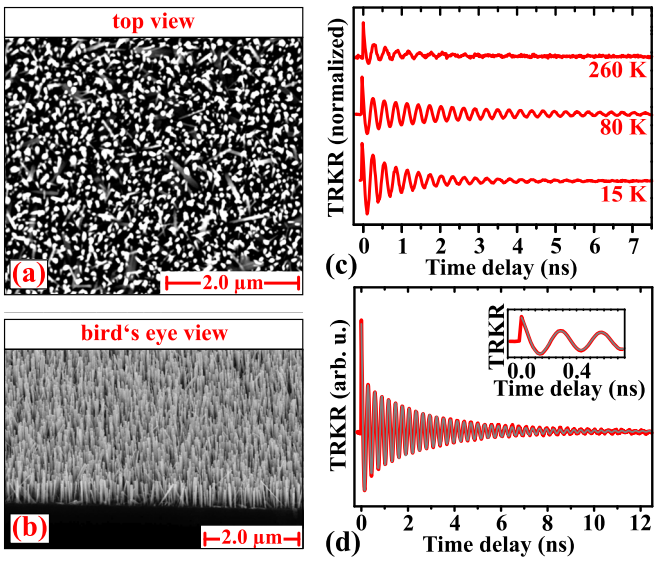

FIG. 1. (a) Top and (b) bird's eye view scanning electron micrographs of the NW ensemble under investigation. (c) TRKR transients for different temperatures in an external magnetic field $B_{\mathrm{ext}} = 0.1$ T. (d) TRKR transient at 80 K together with a fit (grey line) accounting for the decay of the initially excited carrier population. The inset shows the initial decay in more detail.

the decay of the photo-excited carrier density. The corresponding Larmor precession frequency ω_L and spin relaxation time τ_s are extracted by damped cosine fits $[A_1 \exp(-t/\tau_c) + A_2] \exp(-t/\tau_s) \cos[\omega_L(t - t_0)]$ to the TRKR transients [see Fig. 1(d)],[13] where τ_c accounts for the decay of the initially excited charge carrier population.[14] The Larmor precession frequency ω_L shows a perfectly linear magnetic field dependence following $\omega_L = g\mu_B B_{\mathrm{ext}}/\hbar$ with g as the Landé g-factor (not shown), which indicates purely electronic spin dynamics without excitonic contributions.[15] We note that possible excitonic contributions decay very rapidly on a ps time scale due to excitonic recombination and fast excitonic spin relaxation.[16] The electron g-factor obtained from the measured ω_L is compatible with the GaN bulk value[17] $g \approx 1.95$ and shows no temperature dependence within the experimental accuracy (not shown). This insensitivity of the g-factor to temperature changes or confinement effects is expected from $\mathbf{k} \cdot \mathbf{p}$-theory for the combination of a large bandgap and small spin orbit coupling (SOC) in GaN.[17,18]

In the following, we will discuss the temperature dependence of spin relaxation. Figure 2(a) shows the temperature dependence of the spin relaxation time τ_s from $T = 15$ to 260 K at $B_{\mathrm{ext}} = 0.1$ and 1 T. Overall, long spin relaxation times in the ns range are observed, which exceed the spin relaxation times of free, delocalized electrons in bulk GaN by more than an order of magnitude.[13,19,20] The temperature dependence of spin relaxation shows a nonmonotonic behavior, where two regimes of spin relaxation can be clearly distinguished. In the low temperature regime for $T < 100$ K, the spin relaxation time increases with temperature, while in the high temperature regime for $T > 100$ K, a decrease in τ_s with temperature is observed.

The observed nonmonotonic temperature dependence can be explained by the action of two distinctively different spin relaxation mechanisms as we will discuss in the following. At low temperatures, we assume that spin relaxation of localized electrons governs the total spin relaxation, while spin relaxation of delocalized electrons is assumed to dominate at high temperatures. The individual temperature dependencies of these spin relaxation mechanisms lead—in combination with the temperature-dependent degree of localization—to the observed nonmonotonic temperature dependence.

For a quantitative comparison of the experimentally determined spin relaxation times with this model, we plot the temperature dependence of the spin relaxation rate $\gamma_s = 1/\tau_s$ at 0.1 T in Fig. 2(b) on a double-logarithmic scale. At low temperatures, spin relaxation of localized electrons via hyperfine interactions with nuclear spins is assumed to dominate. The nuclear spins act like an effective magnetic field on the electron spin, with fluctuations of this effective magnetic field leading to spin relaxation.[21] The corresponding spin relaxation rate γ_s^{HF} can be approximated by[22,23]

$$\gamma_s^{\mathrm{HF}} = \frac{1}{\hbar}\left(\frac{2\sum_i I_i(I_i+1)A_i^2 y_i}{3N_n}\right)^{1/2}, \tag{1}$$

for non-interacting electrons, where N_n is the number of nuclei overlapping with the electron wavefunction,[24] A_i is the hyperfine constant, I_i is the nuclear spin, and y_i is the abundance of isotope i. A spin relaxation rate $\gamma_s^{\mathrm{HF}} \approx 0.79\,\mathrm{ns}^{-1}$ follows, if an averaged hyperfine constant $A_{\mathrm{Ga}} = 42$ μeV is used for the Ga isotopes ^{69}Ga and ^{71}Ga with $I = 3/2$ and the hyperfine interaction with the nitrogen nuclei is neglected.[25] The estimated value for γ_s^{HF} agrees well with the experimentally observed low temperature value $\gamma_s = 0.86\,\mathrm{ns}^{-1}$ [see also the dashed

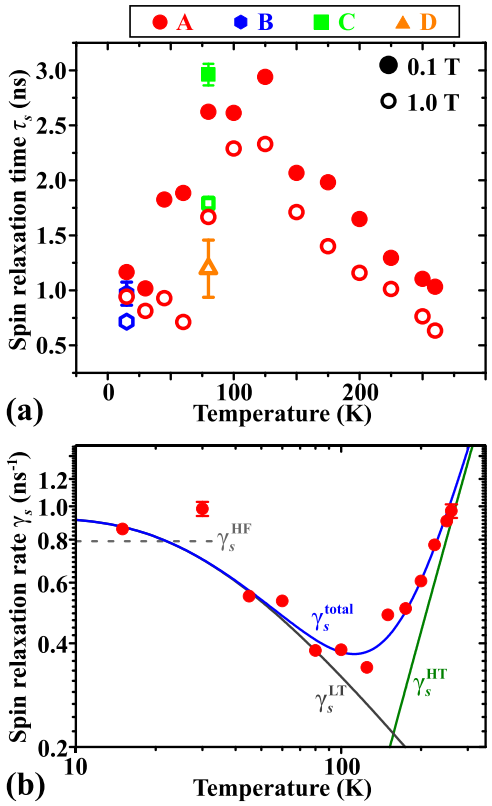

FIG. 2. (a) Temperature dependence of the spin relaxation time τ_s in an external magnetic field of $B_{ext} = 0.1$ T (filled symbols) and 1 T (open symbols) for the NW ensemble under investigation (sample A). Low-temperature values of the spin relaxation time are shown for three additional samples B–D. (b) Temperature dependence of the spin relaxation rate γ_s for sample A at $B_{ext} = 0.1$ T. The lines show a fit of the total spin relaxation rate γ_s^{total} according to Eq. (6) and the corresponding contributions of γ_s^{LT} and γ_s^{HT} of localized and delocalized electrons, respectively.

line in Fig. 2(b)]. The assumption of hyperfine-dominated spin relaxation is also supported by the comparable low-temperature values of the spin relaxation time in three further samples [B–D, see Fig. 2(a)] despite their different NW number densities, NW length, and diameters.[26,39,40]

At high temperatures, DP spin relaxation of delocalized electrons is usually dominating in III–V semiconductors.[6] DP relaxation is based on the combined action of random momentum scattering and spin orbit coupling (SOC), which causes a conduction band spin splitting given by $H_{so} = \frac{\hbar}{2}\mathbf{\Omega}(\mathbf{k}) \cdot \boldsymbol{\sigma}$, with $\boldsymbol{\sigma}$ as the vector of Pauli spin matrices. This spin splitting acts like an effective, wavevector-dependent magnetic field $\mathbf{\Omega}(\mathbf{k})$ on the spins of delocalized electrons. The effective magnetic field forces the electron spins to precess around the effective magnetic field axis. Momentum scattering changes $\mathbf{\Omega}(\mathbf{k})$ randomly, corresponding to fluctuations of the effective magnetic field which randomize the spin for an ensemble of electrons. The tensor of spin relaxation rates follows in a basic approach as[27]

$$\gamma_{s,ij}^{DP} = \frac{1}{2}\left(\delta_{ij}\langle\mathbf{\Omega}^2\rangle - \langle\Omega_i\Omega_j\rangle\right)\tau_p^{eff} \equiv \langle\Omega_{eff}^2\rangle_{ij}\tau_p^{eff}, \tag{2}$$

where $\langle\ldots\rangle$ denotes averaging over the electron momentum distribution and τ_p^{eff} is the effective momentum scattering time. In general, different effects can contribute to the total effective magnetic field $\mathbf{\Omega}_{total}(\mathbf{k}) = \sum_i \mathbf{\Omega}_i(\mathbf{k})$. For NWs with a wurtzite (WZ) structure, contributions due to the inversion asymmetry of the underlying bulk material and due to interface effects are expected.[8] We will start by discussing the effective magnetic field $\mathbf{\Omega}_{wz}(\mathbf{k})$ for bulk wurtzite GaN, which is distinctively different from the effective magnetic field for semiconductors with a zincblende structure,[28] as it includes a term linear in k (Rashba term)[29] and a cubic k^3-term due to the wurtzite bulk inversion asymmetry,[30] corresponding to

$$\mathbf{\Omega}_{wz}(\mathbf{k}) = \frac{2}{\hbar}\left[\gamma_e(bk_z^2 - k_\parallel^2) + \alpha_e\right]\begin{pmatrix} k_y \\ -k_x \\ 0 \end{pmatrix}. \tag{3}$$

Here, γ_e is the Dresselhaus coefficient, b is a structural coefficient, α_e is the Rashba coefficient, $z \parallel [0001]$ (c-axis), $x \parallel [11\bar{2}0]$, $y \parallel [1\bar{1}00]$ and $k_\parallel^2 = k_x^2 + k_y^2$. While DP relaxation in bulk GaN is dominated by the linear Rashba term,[13] spatial confinement in low-dimensional structures can strongly influence DP relaxation. For electrons confined in NWs, three regimes of DP spin relaxation are expected: For extremely narrow NWs with radius R comparable to the Fermi wavelength λ_F, only the lowest subband is occupied, corresponding to a single 1D transport channel. The DP mechanism is completely switched off in this regime. For wider NWs with radius $\lambda_F < R < \ell_e$ between the Fermi wavelength and the elastic mean free path ℓ_e, higher subbands become occupied and DP spin relaxation occurs due to intersubband scattering.[27,31,32] For even wider NWs with radius $\ell_e \ll R < L_{so}$ between the elastic mean free path ℓ_e and the spin orbit length L_{so}, numerous subbands are occupied, corresponding to a diffusive transport regime. The NWs investigated here fall in this last regime of mesoscopic confinement, as they show no quantization effects, but have radii R much smaller than the spin orbit length $L_{so} \approx \hbar\pi/(m^*\alpha_e) \approx 1.3\,\mu$m.[33] This mesoscopic confinement was recently theoretically predicted to lead to strongly suppressed spin relaxation in narrow wurtzite NWs with a peculiar speed-up of spin relaxation up to bulk values for $R \to L_{so}/4$.[34] The strongly suppressed spin relaxation in the diffusive 1D limit was found to be governed by the cubic Dresselhaus term, which is almost negligible for spin relaxation in the bulk. The corresponding spin relaxation rate γ_s^{1D} is predicted to be anisotropic with $\gamma_{s,\perp}^{1D} = \gamma_{s,z}^{1D}/2$ and should show a characteristic cubic T^3-temperature dependence of the effective magnetic field average with

$$\gamma_s^{1D} = Q\frac{m^{*3}}{\hbar^8}(1+b)^2\gamma_e^2(k_BT)^3\tau_p^{eff}, \tag{4}$$

for non-degenerate doping levels, where m^* is the effective electron mass, k_B is the Boltzmann constant, and Q is a numerical factor on the order of one.

A further contribution to the total effective magnetic field $\mathbf{\Omega}_{total}$ can arise from the inversion asymmetry at the NW sidewalls, as was demonstrated for wurtzite GaAs/(Al,Ga)As core/shell NWs.[8] The corresponding effective magnetic field

$$\mathbf{\Omega}_{IIA}(\mathbf{k}) = \frac{2}{\hbar}\begin{pmatrix} 0 \\ -\alpha_\perp k_z \\ \alpha_\parallel k_y \end{pmatrix} \tag{5}$$

is linear in k, with $\alpha_\parallel$ and $\alpha_\perp$ being the spin orbit coupling coefficients governing the strength of the interface-induced field parallel and

perpendicular to the WZ c-axis.[8] Such k-linear contributions to the effective magnetic field lead to a linear T temperature dependence of the effective magnetic field average for non-degenerate electrons, corresponding to an averaged spin relaxation rate $\gamma_s^{\mathrm{IIA}} \propto (k_B T)\tau_p^{\mathrm{eff}}$.

The effective momentum scattering time τ_p^{eff} entering the DP spin relaxation rate [cf. Eq. (2)] depends generally in a complex way on temperature, doping density, and defect density. We therefore model the temperature dependent spin relaxation rate for delocalized electrons by a simple power-law dependence $\gamma_s^{\mathrm{DP,fit}} = \beta T^{\kappa}$ to account for a temperature-dependent momentum scattering time.

In total, both hyperfine-interaction induced spin relaxation of localized electrons and DP spin relaxation of delocalized electrons contribute to the total spin relaxation, which is characterized by a common spin relaxation rate $\gamma_s^{\mathrm{total}}$ due to fast spin exchange.[12,21] The total spin relaxation rate is then given by[35]

$$\gamma_s^{\mathrm{total}} = \gamma_s^{\mathrm{LT}} + \gamma_s^{\mathrm{HT}} = \eta_{\mathrm{loc}}(T)\gamma_s^{\mathrm{HF,fit}} + [1 - \eta_{\mathrm{loc}}(T)]\gamma_s^{\mathrm{DP,fit}}, \quad (6)$$

with $\eta_{\mathrm{loc}}(T)$ as the temperature-dependent degree of localization. We approximate $\eta_{\mathrm{loc}}(T)$ as a simple thermally activated process $\eta_{\mathrm{loc}}(T) = n_{\mathrm{loc}}(T)/n_{\mathrm{total}} = 1 - \exp(-E_b^{\mathrm{eff}}/k_B T)$, where n_{loc} is the density of localized electrons, n_{total} is the total electron density, and E_b^{eff} is an effective binding energy to a localization center.[36]

A fit of Eq. (6) to the experimental spin relaxation rates gives very good agreement with the fit parameters $\gamma_s^{\mathrm{HF,fit}} = (0.93 \pm 0.23)\,\mathrm{ns}^{-1}$, $E_b^{\mathrm{eff}} = (3.7 \pm 1.5)\,\mathrm{meV}$, and $\kappa = 2.6 \pm 0.4$ [cf. Fig. 2(b)]. The value for $\gamma_s^{\mathrm{HF,fit}}$ is in good agreement with the theoretically estimated value γ_s^{HF}, supporting the assumption of hyperfine-induced spin relaxation at low temperatures. The value of the effective binding energy E_b^{eff} is significantly lower than donor ionization energies for Si and O donors in bulk GaN. However, a direct comparison is difficult due to the simplicity of the model employed here, which completely neglects, for example, the densities of states involved. In addition, binding energies can be strongly reduced by surface effects.[37]

The value of the exponent κ alone does not allow to determine the relative strength of the bulk and the interface contribution to the total DP relaxation, as the temperature dependence of the momentum scattering time τ_p^{eff} is not known. Magnetic field dependent measurements give, however, an access to the spatial symmetry of the spin relaxation tensor[19,31] which differs for the two contributions [cf. Eqs. (3) and (5)]. Figure 3(a) shows the magnetic field dependence of the spin relaxation time at $T = 260\,\mathrm{K}$, which is characterized by a pronounced drop from its zero-field value to significantly smaller values for application of a transverse magnetic field $B_{\mathrm{ext}} > 0$. Exactly the opposite behavior with an increase in the spin relaxation time for application of a transverse magnetic field is expected for the contribution due to the wurtzite bulk inversion asymmetry,[8,19] thus ruling out a dominant role of this contribution. The observed drop of the spin relaxation time in a transverse magnetic field has, however, been reported in GaAs/(Al,Ga)As core/shell NWs where it has been attributed to the dominance of the interface-induced contribution to DP relaxation.[8] The dominant role of the interface-induced contribution is further supported by an estimated value for γ_s^{1D} [Eq. (4)] of about $0.02\,\mathrm{ns}^{-1}$,[38,41,42] which is significantly smaller than the spin relaxation rates observed in the experiment, even when taking into account the predicted strong increase in spin relaxation for increasing NW radii $R \rightarrow L_{so}/4$. Finally, with $\kappa = 2.6 \pm 0.4$ from the temperature-dependent measurements above, the predicted linear T dependence of the effective magnetic field average for the interface-induced contribution corresponds to a temperature dependence $\tau_p^{\mathrm{eff}} \propto T^{1.6 \pm 0.4}$ for the effective momentum scattering time. This exponent is compatible with the weak temperature dependence found in spin relaxation measurements in bulk GaN[13] due to the combined action of electron-electron scattering, ionized-impurity scattering, and surface scattering.

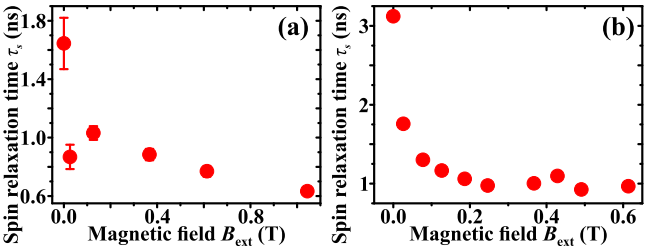

FIG. 3. Magnetic field dependence of the spin relaxation time τ_s for the NW ensemble under investigation at (a) $T = 260\,\mathrm{K}$ and (b) at 15 K for comparison.

To summarize, we have investigated the electron spin dynamics in spontaneously formed GaN NWs for temperatures from 15 to 260 K. The spin relaxation time shows a nonmonotonic temperature dependence which is modeled by a transition from a low temperature regime, where spin relaxation of localized electrons dominates, to a high temperature regime with Dyakonov-Perel relaxation of mesoscopically confined electrons as the dominating mechanism. Magnetic field dependent measurements show that Dyakonov-Perel relaxation is governed by an interface-induced contribution from the NW sidewalls, demonstrating the importance of the high surface-to-volume ratio in these NWs.

We thank J. K. Zettler for the preparation of the samples grown using a two-step process. S. Fernández Garrido acknowledges the partial financial support received through the Spanish program Ramón y Cajal (cofinanced by the European Social Fund) under Grant No. RYC-2016-19509 from Ministerio de Ciencia, Innovación y Universidades.

REFERENCES

[1]G. E. Moore, Electronics **38**, 114 (1965); M. Waldrop, Nature **530**, 144 (2016).
[2]*Spin Physics in Semiconductors*, edited by M. I. Dyakonov (Springer-Verlag, Berlin, 2008); *Semiconductor Spintronics and Quantum Computation*, edited by D. D. Awschalom and N. Samarth (Springer-Verlag, Berlin, 2002).
[3]L. Geelhaar, C. Chèze, B. Jenichen, O. Brandt, C. Pfüller, S. Münch, R. Rothemund, S. Reitzenstein, A. Forchel, T. Kehagias, P. Komninou, G. P. Dimitrakopulos, T. Karakostas, L. Lari, P. R. Chalker, M. H. Gass, and H. Riechert, IEEE J. Sel. Top. Quantum Electron. **17**, 878 (2011).
[4]Y. Huang, X. Duan, Y. Cui, and C. M. Lieber, Nano Lett. **2**, 101 (2002); M. Beeler, P. Hille, J. Schörmann, J. Teubert, M. de la Mata, J. Arbiol, M. Eickhoff, and E. Monroy, *ibid.* **14**, 1665 (2014); F. González-Posada, R. Songmuang, M. Den Hertog, and E. Monroy, *ibid.* **12**, 172 (2012); M. D. Brubaker, P. T. Blanchard, J. B. Schlager, A. W. Sanders, A. Roshko, S. M. Duff, J. M. Gray, V. M. Bright, N. A. Sanford, and K. A. Bertness, *ibid.* **13**, 374 (2013); M. J. Holmes, K. Choi, S. Kako, M. Arita, and Y. Arakawa, *ibid.* **14**, 982 (2014); J. C. Johnson, H.-J. Choi, K. P. Knutsen, R. D. Schaller, P. Yang, and R. J. Saykally, Nat. Mater. **1**, 106 (2002).
[5]J. Tang and K. L. Wang, Nanoscale **7**, 4325 (2015); S. M. Frolov, S. R. Plissard, S. Nadj-Perge, L. P. Kouwenhoven, and E. P. A. M. Bakkers, MRS Bull. **38**, 809 (2013).
[6]M. W. Wu, J. H. Jiang, and M. Q. Weng, Phys. Rep. **493**, 61 (2010).

[7]A. A. Kiselev and K. W. Kim, Phys. Rev. B **61**, 13115 (2000); A. G. Mal'shukov and K. A. Chao, *ibid.* **61**, R2413 (2000).
[8]S. Furthmeier, F. Dirnberger, M. Gmitra, A. Bayer, M. Forsch, J. Hubmann, C. Schüller, E. Reiger, J. Fabian, T. Korn, and D. Bougeard, Nat. Commun. **7**, 12413 (2016).
[9]A. W. Holleitner, V. Sih, R. C. Myers, A. C. Gossard, and D. D. Awschalom, Phys. Rev. Lett. **97**, 036805 (2006); J. Ishihara, M. Ono, Y. Ohno, and H. Ohno, Appl. Phys. Lett. **102**, 212402 (2013); S. Z. Denega, T. Last, J. Liu, A. Slachter, P. J. Rizo, P. H. M. van Loosdrecht, B. J. van Wees, D. Reuter, A. D. Wieck, and C. H. van der Wal, Phys. Rev. B **81**, 153302 (2010); P. Altmann, M. P. Walser, C. Reichl, W. Wegscheider, and G. Salis, *ibid.* **90**, 201306 (2014).
[10]H. Kum, J. Heo, S. Jahangir, A. Banerjee, W. Guo, and P. Bhattacharya, Appl. Phys. Lett. **100**, 182407 (2012); T.-E. Park, Y. H. Park, J.-M. Lee, S. W. Kim, H. G. Park, B.-C. Min, H.-J. Kim, H. C. Koo, H.-J. Choi, S. H. Han, M. Johnson, and J. Chang, Nat. Commun. **8**, 15722 (2017).
[11]J.-Y. Chen, T.-M. Wong, C.-W. Chang, C.-Y. Dong, and Y.-F. Chen, Nat. Nanotechnol. **9**, 845 (2014).
[12]J. H. Buß, J. Rudolph, S. Shvarkov, H. Hardtdegen, A. D. Wieck, and D. Hägele, Appl. Phys. Lett. **102**, 192102 (2013).
[13]J. H. Buß, J. Rudolph, F. Natali, F. Semond, and D. Hägele, Phys. Rev. B **81**, 155216 (2010).
[14]The decay times τ_c agree well with photoluminescence decay times determined by time-resolved photoluminescence measurements (not shown).
[15]D. Hägele, J. Hübner, W. W. Rühle, and M. Oestreich, Phys. B **272**, 328 (1999).
[16]C. Brimont, M. Gallart, O. Crégut, B. Hönerlage, and P. Gilliot, Phys. Rev. B **77**, 125201 (2008).
[17]M. W. Bayerl, M. S. Brandt, T. Graf, O. Ambacher, J. A. Majewski, M. Stutzmann, D. J. As, and K. Lischka, Phys. Rev. B **63**, 165204 (2001).
[18]J. H. Buß, T. Schupp, D. J. As, D. Hägele, and J. Rudolph, J. Appl. Phys. **118**, 225701 (2015).
[19]J. H. Buß, J. Rudolph, F. Natali, F. Semond, and D. Hägele, Appl. Phys. Lett. **95**, 192107 (2009).
[20]J. H. Buß, J. Rudolph, S. Starosielec, A. Schaefer, F. Semond, Y. Cordier, A. D. Wieck, and D. Hägele, Phys. Rev. B **84**, 153202 (2011).
[21]K. V. Kavokin, Semicond. Sci. Technol. **23**, 114009 (2008).
[22]I. A. Merkulov, A. L. Efros, and M. Rosen, Phys. Rev. B **65**, 205309 (2002).
[23]M. Syperek, D. R. Yakovlev, I. A. Yugova, J. Misiewicz, I. V. Sedova, S. V. Sorokin, A. A. Toropov, S. V. Ivanov, and M. Bayer, Phys. Rev. B **84**, 085304 (2011).
[24]The number of nuclei N_n is estimated by the ratio of the electron localization volume to the unit cell volume, assuming a modified Bohr radius $a_e = 1.5\varepsilon_{GaN}/(m^*/m_e)a_H$ and a corresponding volume $V_e = 4/3\pi a_e^3$ for the wavefunction.
[25]B. Urbaszek, X. Marie, T. Amand, O. Krebs, P. Voisin, P. Maletinsky, A. Högele, and A. Imamoglu, Rev. Mod. Phys. **85**, 79 (2013).
[26]Sample B was prepared under identical growth conditions as sample A on which this work focuses. A longer growth time resulted in a NW length of (1000 ± 140) nm, an increased diameter of (54 ± 24) nm, and a reduced NW number density of 1×10^{10} cm^{-2} as a consequence of the increasing degree of coalescence with increasing NW length (Ref. 39). Samples C and D were prepared using a two-step growth process [see Ref. 40], leading to a NW number density of 5×10^9 cm^{-2}, NW length of (280 ± 150) nm, and NW diameter of (35 ± 12) nm for sample C. A higher growth temperature and longer growth time in the second growth step led to a NW number density of 7×10^8 cm^{-2}, NW length of (270 ± 175) nm, and NW diameter of (37 ± 17) nm for sample D.
[27]D. Hägele, S. Döhrmann, J. Rudolph, and M. Oestreich, Adv. Solid State Phys. **45**, 253 (2005).
[28]J. Rudolph, J. H. Buß, and D. Hägele, Phys. Status Solidi B **251**, 1850 (2014).
[29]E. I. Rashba, Sov. Phys. Solid State **2**, 1109 (1960).
[30]W.-T. Wang, C. L. Wu, S. F. Tsay, M. H. Gau, I. Lo, H. F. Kao, M.-E. Lee, Y.-C. Chang, C.-N. Chen, and H. C. Hsueh, Appl. Phys. Lett. **91**, 082110 (2007).
[31]S. Döhrmann, D. Hägele, J. Rudolph, M. Bichler, D. Schuh, and M. Oestreich, Phys. Rev. Lett. **93**, 147405 (2004).
[32]C. Lü, H. C. Schneider, and M. W. Wu, J. Appl. Phys. **106**, 073703 (2009).
[33]Using $m^* = 0.2m_e$ and $\alpha_e = 9.0$ m eV Å, and defining L_{so} as the distance an electron has to travel so that its spin rotates by 2π around the effective magnetic field.
[34]M. Kammermeier, P. Wenk, F. Dirnberger, D. Bougeard, and J. Schliemann, Phys. Rev. B **98**, 035407 (2018).
[35]W. O. Putikka and R. Joynt, Phys. Rev. B **70**, 113201 (2004).
[36]A. Greilich, A. Pawlis, F. Liu, O. A. Yugov, D. R. Yakovlev, K. Lischka, Y. Yamamoto, and M. Bayer, Phys. Rev. B **85**, 121303 (2012).
[37]P. Corfdir, J. K. Zettler, C. Hauswald, S. Fernández-Garrido, O. Brandt, and P. Lefebvre, Phys. Rev. B **90**, 205301 (2014).
[38]Using $\gamma_e = 0.4$ eV Å^3 (Ref. 41) and a mobility of 250 cm^2 V^{-1} s^{-1} (Ref. 42).
[39]V. M. Kaganer, S. Fernández-Garrido, P. Dogan, K. K. Sabelfeld, and O. Brandt, Nano Lett. **16**, 3717 (2016).
[40]J. K. Zettler, P. Corfdir, L. Geelhaar, H. Riechert, O. Brandt, and S. Fernández-Garrido, Nanotechnology **26**, 445604 (2015).
[41]C. Yin, B. Shen, Q. Zhang, F. Xu, N. Tang, L. Cen, X. Wang, Y. Chen, and J. Yu, Appl. Phys. Lett. **97**, 181904 (2010).
[42]Z. Fang, E. Robin, E. Rozas-Jiménez, A. Cros, F. Donatini, N. Mollard, J. Pernot, and B. Daudin, Nano Lett. **15**, 6794 (2015).